

Low-Frequency Representation of Radio-Frequency Absorbers

R. Johnk and J. Randa
Electromagnetic Fields Division
National Institute of Standards and Technology
Boulder, CO 80303

Abstract - We present a simple model to characterize the behavior of radio-frequency absorbers at low frequency. The absorber is represented by a flat, homogeneous, isotropic slab of lossy material, with effective constitutive parameters. These parameters are determined by a fit to measured data. Excellent fits are obtained in the two applications considered. The model is intended for use in the characterization of absorber-lined chambers at low frequency. It could also be used to predict the low-frequency performance of partially loaded shielded enclosures.

INTRODUCTION

The low-frequency behavior of RF absorber and absorber-lined chambers (ALC) is of considerable interest and has received a corresponding amount of attention in the EMC community (see, e.g., [1-12]). This is because the performance of ALCs deteriorates at low frequency (typically somewhere between 50 MHz and 500 MHz), where many EMC tests must be done. Since ALCs are often used for EMC testing, it is important that their low-frequency (below about 500 MHz) behavior be characterized and understood.

This paper presents a model for representing the electromagnetic properties of a wall of RF absorber at low frequency. A more detailed account is contained in [13]. The motivation was to develop a simple model whose free parameters can be determined by fits to measured reflection coefficients, and which could then be used to represent the walls of an ALC in calculations predicting chamber performance. The original intention was to use the model in a modal calculation of ALC fields, but it could also be used to represent the walls in other approaches, for example, a finite-difference computation of chamber fields. In this paper we present the first step of the process: we describe the model and show that it does a good job representing the scattering properties of an absorbing wall. We do not present calculations of full ALC behavior.

THE MODEL

Physical Model

The specific model we use to represent the wall of absorber at low frequency consists of a flat slab of uniform, isotropic, lossy material, backed by a perfect conductor. This is represented in fig. 1. The approximation of using a flat surface is motivated by the fact that structure much smaller than a wavelength cannot be resolved by the incident wave. The relative permittivity ϵ , conductivity σ , and thickness d of the slab are left as free parameters, to be determined by a fit to reflection coefficient data. In this paper we take the effective permeability of the absorber to be that of free space, $\mu = \mu_0$. As will be evident below, the model could also be applied to ferrite tiles, in which case the permeability would be treated as an additional free parameter. The parameters of the model are not the actual physical permittivity, conductivity, and

thickness of the foam absorber. Instead they are effective parameters of the flat slab, which include effects from the size and shape of the absorbing cones. Nevertheless, we expect the effective parameters to be physically "reasonable"; if they are wildly different from the actual physical values, the model is suspect. If a good fit to all relevant data can be obtained with physically reasonable values of the parameters, then we have a simple representation for the absorbing wall at low frequency, which can be used in constructing a model of an ALC, a semi-anechoic chamber, or a partially loaded shielded enclosure. (It cannot be used as a tool for absorber design: it reproduces measured absorber behavior; it does not predict it.)

The reflection coefficient in this model is calculated by a straightforward exercise in boundary matching, with a little care required for the lossy medium. (For details see [13].) The results are

$$R_{TE} = \frac{E_r}{E_i} = \frac{\mu \omega \cos \theta + j \eta_0 \gamma_z \coth(\gamma_z d)}{\mu \omega \cos \theta - j \eta_0 \gamma_z \coth(\gamma_z d)}, \quad (1)$$

$$R_{TM} = \frac{H_r}{H_i} = \frac{(\sigma + j \omega \epsilon) \eta_0 \cos \theta - \gamma_z \tanh(\gamma_z d)}{(\sigma + j \omega \epsilon) \eta_0 \cos \theta + \gamma_z \tanh(\gamma_z d)}, \quad (2)$$

for the (field) reflection coefficients for transverse electric and transverse magnetic polarization of the incident wave, where the geometric configuration is shown in fig. 2. In these equations, μ is the permittivity of the slab, ω is the angular frequency, θ is the angle of incidence, η_0 is the wave impedance of free space, and γ_z is the complex propagation constant, which is a (known) function of ω , μ , ϵ , σ , and θ .

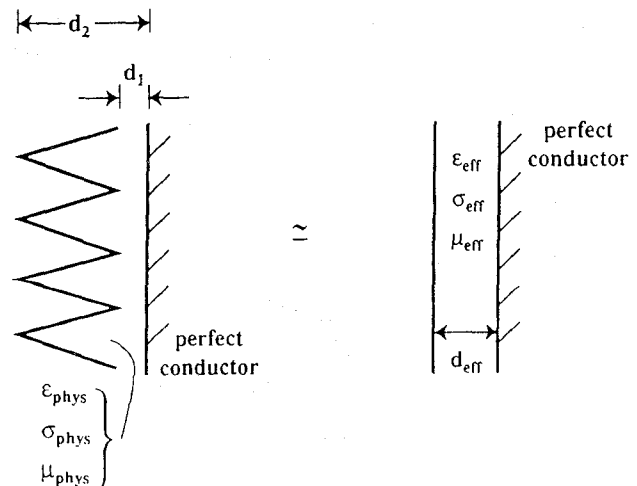


Fig. 1 Approximation of replacing absorbing cones with conducting back plane by a lossy slab with a conducting back plane.

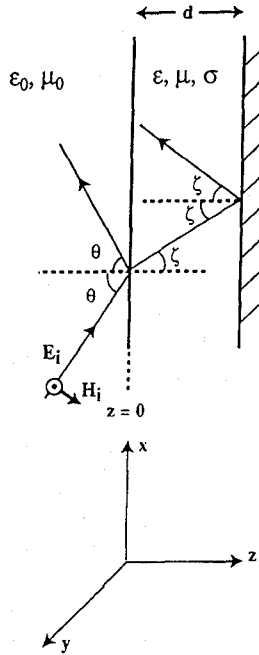


Fig. 2 Plane wave incident on lossy slab.

Fitting Procedure

The free parameters in eqs. (1) and (2) are to be determined by fits to experimental data. All fits and statistics were done on the amplitude $|R_{TE}|$, but the results will be presented in decibels. Performing the fits on $|R_{TE}|^2$ or on the decibel value changes the results only slightly. To perform the fits we used an orthogonal distance regression (ODR) package developed by the NIST Computing and Applied Mathematics Laboratory [14]. As applied in this paper, the ODR procedure is a simple generalization of the ordinary least squares (OLS) fitting procedure. In an OLS fit the residuals are defined as the differences between the fitting function and the measurements at the same frequency, and one minimizes the weighted sum of the residuals squared, which we denote χ_{OLS}^2 ,

$$\chi_{OLS}^2 = \sum_i [y_i - y(f_i; \beta)]^2 w_i, \quad (3)$$

$$w_i = \frac{1}{\sigma_i^2},$$

where y_i are the measurement results, f_i are the measurement frequencies, $y(f, \beta)$ is the fitting function, β represents the free parameters, and the weights w_i are typically taken to be the inverses of the squared standard deviations of the measurements. The ODR procedure defines the residuals as the orthogonal distances between measurement points and fitting curve, thereby allowing for some uncertainty in the measurement frequency. The function to be minimized is

$$\chi_{ODR}^2 = \sum_i (w_{yi} [y_i - y(f_i + \delta_i; \beta)]^2 + w_{fi} \delta_i^2), \quad (4)$$

$$w_{yi} = \frac{1}{\sigma_{yi}^2}, \quad w_{fi} = \frac{1}{\sigma_{fi}^2},$$

where σ_{yi} and σ_{fi} are the standard deviations in the measurements of y and f . The data in this paper were

all obtained from FFT's of time domain measurements [11, 12], and thus each point represents an average over a significant frequency range (20 MHz) rather than a measurement at one frequency with negligible bandwidth. Consequently an ODR fit is more appropriate for our purposes than OLS. There is not much difference between the two in the examples below, but we will present ODR results. If the weights w_i are taken to be the inverses of the squared standard deviations (of the means) in eqs. (3) and (4), then the quantity χ^2 provides a measure of how good the fit is. A correct theory will usually result in $\chi^2/\nu \leq 1$, where ν is the number of degrees of freedom, defined as the number of measurement points minus the number of fitting parameters. (Those unfamiliar with fitting procedures and significance are referred to references such as [15, 16].)

Two of our effective parameters, σ and ϵ , are frequency dependent. We parameterize this dependence as

$$\frac{\epsilon(f)}{\epsilon_0} = 1 + \hat{\epsilon}_{100} \left(\frac{f}{f_0} \right)^{\alpha_\epsilon}, \quad (5)$$

$$\sigma(f) = \sigma_{100} \left(\frac{f}{f_0} \right)^{\alpha_\sigma},$$

where $f_0 = 100$ MHz. Thus $(1 + \hat{\epsilon}_{100})$ and σ_{100} are the values at 100 MHz, and α_ϵ and α_σ control the frequency dependence. This functional form was chosen for simplicity and convenience; it does not have a physical justification. Indeed, since the frequency dependence of these effective parameters must in some way include the frequency dependent effects of the absorber cones, a physical derivation of the frequency dependence would be quite complicated. In principle, the effective thickness d could also have a frequency dependence, but it is not required in our applications, and so we do not include it. We then have five free parameters to determine from the measured data: $\hat{\epsilon}_{100}$, α_ϵ , σ_{100} , α_σ , and d . Given a set of measurement results we vary these five parameters (within physically reasonable values) to obtain the best agreement with the data. If the minimum χ^2 corresponds to $\chi^2/\nu < 1$ where ν is the number of degrees of freedom, then our model agrees with the measured results as well as a full, correct calculation could be expected to agree. Stated another way, the measurements do not distinguish between our model and the full, correct theory.

SMALL-ABSORBER APPLICATION

The first application we consider is to data [17] taken on a small (29.2 cm thick), pyramidal, polyurethane foam absorber, depicted in fig. 3. The sample used in the measurements was a 2.44 m (8 ft) square. The measurements were made at normal

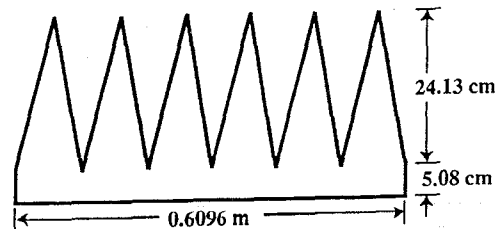


Fig. 3 Small absorber used in first application of model.

incidence, using the time-domain technique described in [11]. The conversion to the frequency domain introduces a frequency bin size of 20 MHz. Three separate measurements were made, using three different combinations of distances for the transmitting and receiving antennas. From the three measurements we computed an average and standard deviation (using the amplitudes, then converting the results to decibels) at each frequency. The effective parameters for this absorber are determined by fitting the magnitude of the reflection coefficient, determined from eq. (1), to the data. In performing the fits we used the full standard deviations, including both type-A and type-B uncertainties [18] (both statistical and systematic). In the figures the error bars will correspond to only the statistical, type-A, uncertainties. The type-B uncertainty is about 20% of the measured value of the reflection coefficient. It is not shown because its primary effect is on the overall normalization, whereas our interest in the fits is on the shape or point-to-point variations.

There are two aspects of the experimental data, which invite the injection of some scientific judgment. The first is that $|R|$ exceeds 0 dB at low frequency; that is, more power is reflected than was incident. This unphysical result is an artifact of the measurement method, explained in [11], and we do not want it to influence our fit. Therefore, for points at which $|R| > 0$ dB, we set $|R| = 0$ dB in the fitting routine. The second questionable feature of the data is the behavior around 400 MHz. If we include all those points, the fitting routine attempts to produce a bump around 400 MHz, which does not occur naturally in the model. The result is a poor fit and unrealistic parameter values. In the time-domain method used in the measurements, a spurious structure could have been produced through a conspiracy of inopportune distances, small signals, and the FFT. (This pathology was remedied in later measurements.) We therefore did not include the four data points at 380–440 MHz in our fits, though we will show them in our comparisons of fits to data. If the structure around 400 MHz proves to be real, our simple model is incapable of reproducing it.

A final consideration in performing the fit is the appropriate frequency range. The model can be expected to fail for frequencies at which the

wavelength is comparable to or smaller than characteristic (electrical) lengths of the absorber. In this case the relevant length is twice the thickness of the slab. Due to the taper of the cones, there is a longitudinal dependence of the effective permittivity [3,6] which is neglected in our model; and when the wavelength in the material becomes comparable to $2d$, these effects become important. Although we do not know d or $\epsilon(f)$ before the fit, the position of the dip tells us the electrical distance in the slab. In the model the first prominent dip is caused by the destructive interference between the waves reflected from the front surface and the back wall. Thus, at the dip frequency the wavelength in the material is about $4d$, and we can expect the model to break down somewhere in the neighborhood of the first prominent dip, which for this absorber occurs at about 580 MHz.

For frequency ranges up to about 600 or 700 MHz, the ODR routine has no trouble finding good fits to the measured data. Indeed, by using different initial values of the parameters, we can find many different sets of "optimized" parameters, corresponding to different local minima of the optimization function, eq. (4). An important point is that we are not necessarily seeking the absolute minimum of the function χ^2 . We are more interested in a good fit with realistic parameters than in a slightly better fit with unrealistic values of the parameters. We have found that the most effective way to focus on realistic parameter values is to restrict our search to solutions with thickness d between 0.05 m and 0.29 m, since these are the relevant thicknesses of the absorber (see fig. 3). Good fits were found for $0.05 \text{ m} \leq d \leq 0.17 \text{ m}$, but fits for $d < 0.08 \text{ m}$ or $d > 0.15 \text{ m}$ had unpalatably large values of $\hat{\epsilon}_{100}$ and/or α_c . We therefore narrow the range of good fits to $0.08 \text{ m} \leq d \leq 0.15 \text{ m}$. For our preferred fit we choose a thickness near the midpoint of the range. The parameter values of the preferred fit are $d = 0.12 \text{ m}$, $\epsilon_{100} = 41.30$, $\alpha_c = 2.427$, $\sigma_{100} = 0.009963 \text{ S/m}$, and $\alpha_g = 0.8008$. The curve resulting from using these values in eqs. (3), (5) is compared to the data in fig. 4. All the data are plotted in the figure, not just those used in the fit. The error bars correspond to one standard deviation of the statistical (Type-A) error only, $\pm\sigma_{Ai}$. Horizontal error bars are not shown because they are all the same and small ($\pm 5 \text{ MHz}$). The agreement is

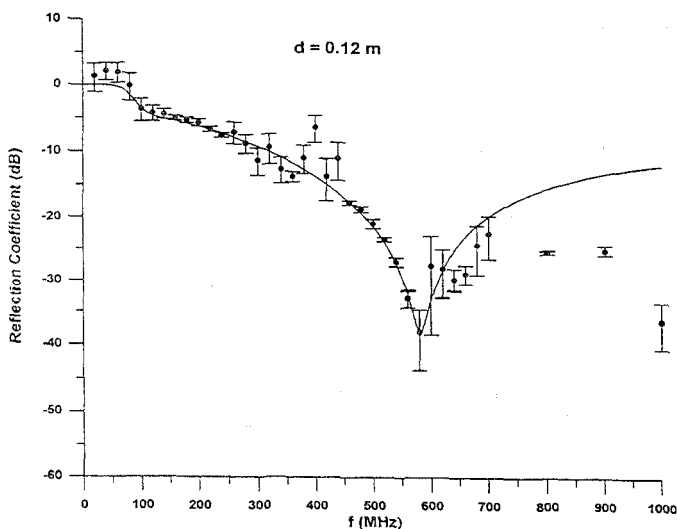


Fig. 4 Preferred fit to small-absorber data over 0–580 MHz frequency range.

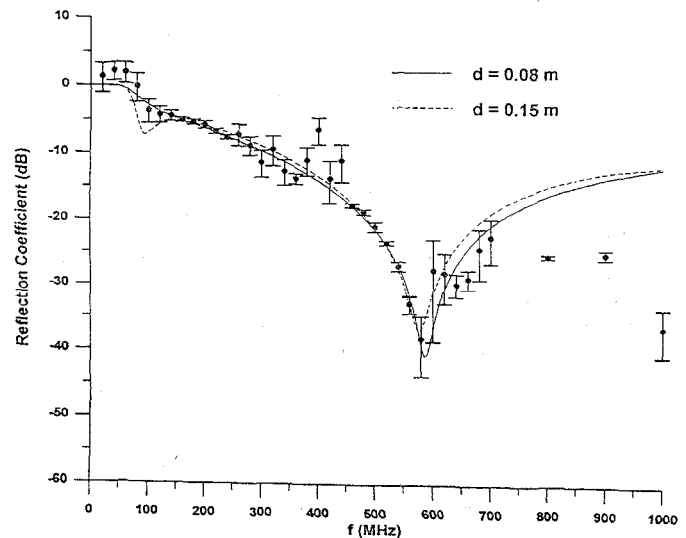


Fig. 5 Other acceptable fits to small-absorber data.

excellent over the range of the fit (0–580 MHz), and it remains moderately good up to about 700 MHz. To quantify the agreement we note that χ_{ODR}^2 is 2.5 with 20 degrees of freedom, which is embarrassingly good. Even if we include the points near 400 MHz, neglect any type-B contribution to the total standard deviation, and compute χ_{OLS}^2 , we obtain $\chi_{OLS}^2/\nu = 0.44$ over the 20–580 MHz range, which still represents very good agreement.

We thus have a very accurate representation of this absorber up to about 600 MHz. It would also be useful to know the uncertainty in the determination of the effective parameters. As noted above, there are good fits with acceptable values of the parameters for $0.08 \text{ m} \leq d \leq 0.15 \text{ m}$. The solutions at the ends of this interval are $d = 0.08 \text{ m}$, $\hat{\epsilon}_{100} = 91.29$, $\alpha_e = 2.164$, $\sigma_{100} = 0.012 \text{ S/m}$, $\alpha_g = 0.9409$, and $d = 0.15 \text{ m}$, $\hat{\epsilon}_{100} = 22.92$, $\alpha_e = 2.849$, $\sigma_{100} = 0.014 \text{ S/m}$, $\alpha_g = 0.4439$. The curves for these two solutions are compared to the data in fig. 6, and both agree very well. Therefore, in using this model in a calculation, one would also evaluate the result using the $d = 0.08 \text{ m}$ and $d = 0.15 \text{ m}$ solutions, in order to gauge the sensitivity of the calculation to the model parameters.

The exclusion of fits with unacceptable values for one or more parameters warrants comment. Solutions with unrealistic values of the parameters are suspect on the grounds that the parameters may be delicately balanced to produce a fit which agrees with the input data, but produces highly improbable predictions in other places, for example, at different frequencies or in other measurable quantities. The present model is intended to represent all (macroscopic) facets of the electromagnetic behavior of the absorber, and so we want to minimize the likelihood of nasty surprises. Avoiding unrealistic parameter values is one way to do so. Further discussion of this point, including an example, can be found in [13].

APPLICATION TO MIDSIZE ABSORBER

The second example is absorber 3 of [11]. It is a fire retardant absorber, 0.91 m tall, with twisted pyramids, fig. 6. The test sample was a 3 m square. Additional measurements were made on this absorber

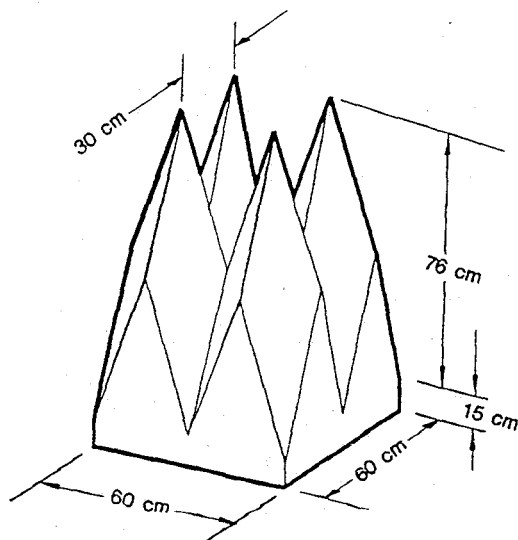


Fig. 6 Mid-size absorber used in second application.

after publication of [11], and we now have three different measurements at each frequency. We also present more frequency points than previously published. As in the first example, the three measurements are used to compute an average and standard deviation. In this case there are no obvious anomalies requiring special treatment. Fits were performed using both the full standard deviations and using just the statistical standard deviation computed from the three measurements. We will present the fits obtained using just the statistical standard deviations. Drawing on the experience of the last example, we chose the frequency range to extend to 300 MHz, just beyond the first prominent dip.

The absorber dimensions suggest that the effective thickness d should be between 0.15 m and 0.91 m. We scanned this entire region and were able to find good fits for $0.37 \text{ m} \leq d \leq 0.55 \text{ m}$. Fits with d less than about 0.40 m have a very deep, sharp dip between 20 and 40 MHz, and consequently we discarded them. Figure 7 compares the fitted curve to the data for the best fit, $d = 0.4368 \text{ m}$, $\hat{\epsilon}_{100} = 69.08$, $\alpha_e = 2.049$, $\sigma_{100} = 0.018 \text{ S/m}$, $\alpha_g = -0.4267$. The agreement is very good, as is reflected by the fact that $\chi_{ODR}^2/\nu = 0.27$, using just statistical standard deviations. If we wish to avoid negative values of α_g , we can fix $\alpha_g = 0$. Then the best fit is for $d = 0.4568 \text{ m}$, $\hat{\epsilon}_{100} = 63.31$, $\alpha_e = 2.062$, $\sigma_{100} = 0.01267 \text{ S/m}$, for which $\chi_{ODR}^2/\nu = 0.89$.

There are also data for the angular dependence of the reflection coefficient for this absorber [12]. (Again, what is measured is an approximation to the true reflection coefficient.) Because the time windowing was different for the bistatic angular measurements (front surface reflection as opposed to full reflection), we did not include these data in the fit described in the preceding paragraph. We can compare calculated results to angular data using the fitted values for the effective parameters, but there is a minor difficulty in doing so. The $\theta=0$ bistatic data do not agree exactly with the monostatic data. Since the model was constrained to agree with the monostatic data, its overall normalization will not be correct for the bistatic (angular) data. This is seen in figs. 8a and 8b, where the dashed curves are the model calculations using the parameters noted above ($d = 0.4368 \text{ m}$, etc.). The vertical error bars on the data correspond to $\pm 2 \text{ dB}$ [12], whereas the horizontal error bars reflect the size of the angular bins. For

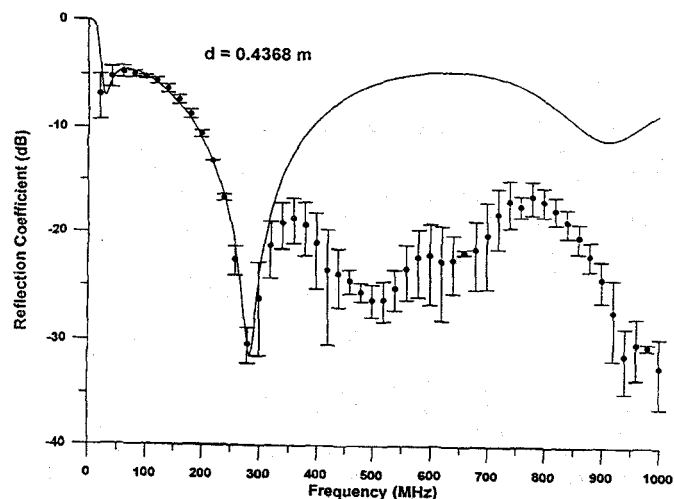


Fig. 7 Preferred fit, over 0–300 MHz range, to data for midsize absorber.

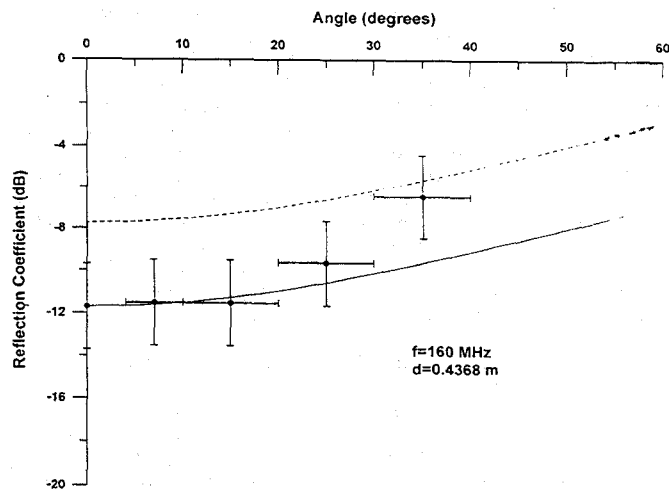


Fig. 8a Predicted curves for angular dependence of reflection coefficient at 160 MHz. Solid curve has been normalized to take into account the discrepancy between monostatic and bistatic data.

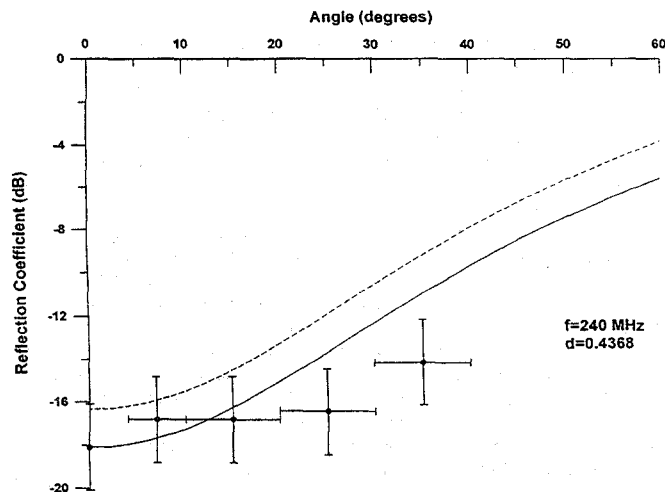


Fig. 8b As in fig. 8a, for 240 MHz.

purposes of comparing the shape of the angular calculations to the data, we have also plotted a solid curve which is the model calculation normalized to agree with the angular data at $\theta=0$, as it would if bistatic and monostatic measurements agreed exactly. The agreement for the two representative frequencies shown is quite satisfying and offers additional evidence for the basic validity of the model.

SUMMARY AND CONCLUSIONS

We have presented a simple model for representing the low-frequency behavior of absorbing materials backed by a conducting wall. The model does not enable one to calculate absorber properties from geometrical and material properties, and therefore it is not an absorber design tool. It is intended instead as a way to incorporate measured properties of absorbers in calculations of the performance of chambers lined entirely or partially with those

absorbers. (It could also provide a simple parameterization of calculated properties.) The model was applied to two absorbers of different sizes and shapes and was able to replicate the behavior of their reflection coefficients up to a frequency slightly above the first prominent minimum in each case. The two examples considered were polyurethane foam, but the model should also be applicable to ferrite or composite absorbers. There are two principal advantages of the model. One is its simplicity, which should permit its use as the basis of relatively realistic and detailed calculations of field structure within absorber-lined chambers. The other advantage is that (by construction) it accurately reproduces the measured reflection properties of walls of absorbing material. Of course, this is an advantage only if one has good measurements of the reflection properties. The limitations of the model are the restriction to low frequency and the general limitations shared by any model relying on empirical fits to determine effective parameters: it is only as good as the input data; difficulties could in principle arise in other physical quantities which were not included in the fit; etc.

ACKNOWLEDGMENTS

We are grateful to Paul Domich for assistance in using the ODR package, to Andy Ondrejka for discussions on the time-domain measurement methods, and to Chris Holloway for comments and suggestions. We are also grateful to Andy Ondrejka and Santi Tofani for providing their unpublished data.

REFERENCES

- [1] L. Farber and H. R. Hofman, "Correlation of theoretical and measured site attenuation in an absorber-lined chamber," in *Proc. 1983 IEEE Int. Symp. on EMC* (Arlington, VA), August 1983, pp. 492-497.
- [2] S. R. Mishra and T. J. F. Pavlasek, "Design of absorber-lined chambers for EMC measurements using a geometrical optics approach," *IEEE Trans. Electromagn. Compat.*, vol. EMC-26, no. 3, pp. 111-119, Aug. 1984.
- [3] E. F. Kuester and C. L. Holloway, "Improved low-frequency performance of pyramid-cone absorbers for applications in semi-anechoic chambers," in *Proc. 1989 IEEE Nat. Symp. on EMC* (Denver, CO), May 1989, pp. 394-399.
- [4] P. Wilson, H. Garbe, and D. Hansen, "A simulation of site attenuation in anechoic chambers: try before you buy," in *Proc. 9th Int. Zurich Symp. on EMC* (Zurich, Switzerland), March 1991, pp. 311-316.
- [5] J. Jarem, "Electromagnetic field analysis of a four-wire anechoic chamber," *IEEE Trans. on Antennas and Propagat.*, vol. 38, no. 11, pp. 1835-1842, Nov. 1990.
- [6] E. F. Kuester and C. L. Holloway, "Plane-wave reflection from inhomogeneous uniaxially anisotropic absorbing layers," Univ. of Colorado, Electromagnetics Laboratory, Scientific Report No. 97, Boulder, CO, May 1989.
- [7] C. Cheon and V. Liepa, "Full wave analysis of infinitely periodic lossy wedges," in *Proc. 1990 IEEE Antennas and Propagation Symposium* (Dallas, TX), May 1990, pp. 618-621.
- [8] R. Janaswamy, "Oblique scattering from lossy periodic surfaces with application to anechoic chamber absorbers," *IEEE Trans. Antennas and Propagat.*, vol. 40, no. 2, pp. 162-169, Feb. 1992.

- [9] C.-F. Yang, W. D. Burnside, and R. C. Rudduck, "A doubly periodic moment method solution for the analysis and design of an absorber covered wall," *IEEE Trans. Antennas & Propagation*, vol. AP-41, no. 5, pp. 600-609, May 1993.
- [10] N. Marly, D. DeZutter, L. Martens, and H. Pues, "A surface integral equation approach to the scattering and absorption of doubly periodic lossy structures," *IEEE Trans. on EMC*, vol. EMC-36, no. 1, pp. 14-22, Feb. 1994.
- [11] S. Tofani, A. Ondrejka, and M. Kanda, "A time-domain method for characterizing the reflection coefficient of absorbing materials from 30 to 1000 MHz," *IEEE Trans. EMC*, vol. EMC-33, no. 3, pp. 234-240, Aug. 1991.
- [12] A. Tofani, A. R. Ondrejka, M. Kanda, and D. A. Hill, "Bistatic scattering of absorbing materials from 30 to 1000 MHz," *IEEE Trans. on EMC*, vol. EMC-34, no. 3, pp. 304-307, Aug. 1992.
- [13] J. Randa, "Low-frequency model for radio-frequency absorbers," *J. Res. Natl. Inst. Stand. Technol.* 100, pp. 257-267 (1995).
- [14] P. T. Boggs, R. H. Byrd, J. E. Rogers, and R. B. Schnabel, "User's reference guide for ODRPACK version 2.01; Software for weighted orthogonal distance regression," *Nat. Inst. Stand. Technol.*, Internal Report NISTIR-4834, June 1992.
- [15] P. R. Bevington, *Data Reduction and Error Analysis for the Physical Sciences*. New York: McGraw-Hill, 1969, ch. 10.
- [16] W. H. Press, B. P. Flannery, S. A. Teukolsky, and W. T. Vetterling, *Numerical Recipes*. Cambridge, U.K.: Cambridge University Press, 1986, ch. 13 and 14.
- [17] A. Ondrejka and R. Johnk, unpublished.
- [18] B. N. Taylor and C. E. Kuyatt, "Guidelines for evaluating and expressing the uncertainty of NIST measurement results," *Nat. Inst. Stand. Technol.*, Tech. Note TN1297, January 1993.